Recombinant *h*IFN-α2b-BCG inhibits tumor growth in a mouse model of bladder cancer

ERLIN SUN[1*], XIAODONG FAN[2*], LINING WANG[1], MINGDE LEI[1], XIAODONG ZHOU[1], CHUNYU LIU[1], BINGXIN LU[1], XUEWU NIAN[1], YAN SUN[1] and RUIFA HAN[1]

[1]Department of Urology, Tianjin Institute of Urology, The Second Hospital of Tianjin Medical University, Tianjin 300211; [2]Department of Gynaecology, Tianjin City Hospital for Gynaecology and Obstetrics, Tianjin 300100, P.R. China

Received January 14, 2015; Accepted April 20, 2015

DOI: 10.3892/or.2015.3985

Abstract. Bacillus Calmette-Guérin (BCG) reduces the recurrence and progression of non-muscle invasive bladder cancer. The present study aimed to investigate the impact of a recombinant *h*IFN-α2b-secreting BCG (*r*BCG) on the mouse bladder MB49 cell line and an orthotopic mouse model of bladder cancer. MB49 cells were cultivated in the presence or absence of *r*BCG, BCG or BCG+*h*IFN-α2b. Cellular morphology and viability were assessed by microscopy and CCK-8 assay, respectively. Apoptosis was assessed by acridine orange, Hoechst 33258 staining and flow cytometry. MHC-I expression was assessed by flow cytometry. MB49 cells were transplanted into the bladders of C57BL/6 mice administered BCG, *r*BCG or BCG+*h*IFN-α2b. Local tissue Fas expression and T cell subsets were assessed by immunohistochemistry. Peripheral blood TNF-α and IL-12 levels were measured by ELISA, and circulating T lymphocyte subsets by flow cytometry. BCG, *r*BCG and BCG+*h*IFN-α2b increased the distortion and death of MB49 cells, yet *r*BCG reduced the proliferation and enhanced apoptosis most substantially. Apoptosis was increased after a 24-h co-culture with rBCG or BCG+*h*IFN-α2b. Mice administered *r*BCG survived longer than mice administered BCG ($p<0.001$), yet this result was not significantly different from mice administered BCG+*h*IFN-α2b. The average bladder weight was reduced by administration of *r*BCG ($p<0.001$). Fas expression and peripheral blood *m*TNF-α and *m*IL-12, cell counts of polymorphonuclear leukocytes, monocytes, T lymphocytes and $CD4^+/CD8^+$ ratios were significantly increased by all BCG treatments ($p\leq0.05$), yet monocyte and T lymphocyte counts were higher in mice administered rBCG than in mice treated with BCG or BCG+*h*IFN-α2b ($p=0.000$). These results indicate that in an orthotopic murine bladder cancer model *r*BCG possesses superior antitumor activity to BCG+*h*IFN-α2b.

Correspondence to: Dr Erlin Sun or Dr Ruifa Han, Department of Urology, Tianjin Institute of Urology, The Second Hospital of Tianjin Medical University, Tianjin 300211, P.R. China
E-mail: irene_sunsun@yahoo.com
E-mail: ruifahan@gmail.com

*Contributed equally

Key words: Bacilli Calmette-Guérin, recombinant BCG, *h*IFN-α2b, bladder tumor, immunotherapy, murine orthotopic bladder cancer, apoptosis

Introduction

The global prevalence of bladder cancer is estimated at more than 1 million and is steadily increasing. At diagnosis, 20-25% of cases are non-muscle invasive bladder cancer (NMIBC), and there is a high rate of tumor recurrence and progression even after local surgical therapy. Thus, numerous patients require lifelong follow-up examinations that include additional prophylactic treatments in the event of recurrence. Intravesical Bacillus Calmette-Guérin (BCG), a live attenuated *Mycobacterium bovis* vaccine widely used to induce immunity against tuberculosis, is currently the most common therapy employed for NMIBC, best known as the most effective agent for the treatment of high-grade superficial bladder cancer. As an adjunct to transurethral resection, BCG is the treatment of choice for urothelial carcinoma *in situ* (CIS) and for recurrent or multi-focal Ta and high grade T1 bladder lesions (1). In patients for whom radical cystectomy is not performed, BCG is currently the first treatment option for high-risk NMIBC and CIS. BCG therapy achieves 50-60% effectiveness against small residual tumors, and a 70-75% complete response rate for CIS (2). Recent trials indicate that immunotherapy with BCG is superior to chemotherapy in patients with intermediate- to high-risk for recurrence (3).

Despite therapeutic application since 1976, the mechanism of BCG action against bladder cancer remains unknown, yet it is assumed that BCG-induced antitumor activity is dominated by local non-specific immunological reactions reflecting the activity of immunocompetent T cells (4). BCG accumulates near and adheres to the bladder wall by binding to fibronectin (5). After passage through the GAG layer, BCG is internalized and processed by professional APC and tumor cells, which then locally activate numerous lymphocytes, macrophages, pleomorphic mononuclear and NK cells (6,7). Th1-polarized cell-mediated immunity appears to play a key role during BCG immunotherapy and IFN-γ-producing, NK

and $CD8^+$ in addition to $CD4^+$ T cells are major cellular mediators of this antitumor action (3).

However, a high percentage of patients fail initial BCG therapy, and 40-50% of BCG responders develop recurrent tumors within the first 5 years (8). In addition, BCG, a viable living organism, causes infections. Unfortunately, up to 90% of patients experience side-effects ranging from bothersome cystitis in the majority of patients to life-threatening complications such as sepsis in rare cases (9). Where BCG is ineffective, treatment schedules consisting of viable BCG and human lL-2 or other Th1 cytokines are proven to be effective (10). Induction of Th1 immunity is required for successful BCG immunotherapy of bladder cancer. The Th1 cytokine *h*IFN-α has been found to be safe and tolerable when administered intravesically, alone or in combination with BCG, in numerous controlled studies (11,12). Additionally administration of IFN-α2b, both alone and in combination with BCG, has been reported to achieve improved clinical efficacy (13). The side-effect profile of combination therapies is similar to BCG monotherapy, and one phase III study has recommended combination therapy with BCG and IFN-α in BCG non-responders or relapsers (14). Although BCG and IFN-α combination therapy may benefit patients with high-risk disease or carcinoma *in situ*, the efficacy of cytokine perfusion is limited by the high cost, short half-life and water solubility of cytokines, which are readily lost to urine (15).

BCG has also been used as a live vehicle to deliver multiple pathogen antigens due to the high immunogenicity and low toxicity of this organism (16). We thus sought to assess the efficacy of administration of a previously described genetically engineered recombinant *h*IFN-α2b-secreting BCG (*r*BCG) (17) in a murine model of bladder cancer.

Materials and methods

BCG strains and culture. The *Mycobacterium bovis (M. bovis*) BCG *Danish* 2 strain was purchased from the Shanghai Institute of Biological Products. Recombinant *h*IFN-α2b-BCG was constructed in-house. The *h*IFN-α2b fragment was directionally cloned into the shuttle plasmid *pMAO-4* to form a recombinant plasmid *phIFN-α-2B*, which was extracted prior to enrichment in DH5α-*E. coli* and electrically transduced into BCG as previously described (17) (Fig. 1). BCG was recovered on 7H10 solid media, and cultured in Middlebrock 7H9 broth media (both from Difco Laboratories, USA) supplemented with 0.05% (by vol) glycerol, 10% (by vol) albumin-dextrose-catalase (ADC) and 0.05% (by vol) Tween-80, at 37˚C and 150 rpm until the log-stationary phase. *r*BCG was supplemented with 15 μg/ml kanamycin (Sigma-Aldrich, St. Louis, MO, USA), and then washed and dissolved in phosphate-buffered saline (PBS). When A_{60} = 1, BCG/*r*BCG in the present study was ~$1.4x10^8$ CFU/ml. Exogenous recombinant IFN-α2b (Sigma-Aldrich) was applied by the same amount of *r*BCG in the 7-day culture supernatant: ~1,000 IU in ~$3x10^8$ CFU/ml.

Bladder cancer cell line and culture. The mouse bladder tumor cell line MB49, originating from the C57BL/6 mouse, was provided by Luo Yi of the Department of Urology, University of Iowa, USA. Cells were grown in RPMI-1640 medium (Gibco, USA) supplemented with 10% fetal bovine serum, at 37˚C in 5% CO_2 in a humidified incubator. Cells in the logarithmic growth phase were seeded at $1x10^6$/ml, and at 90% confluency were co-cultured with BCG or *r*BCG at an MOI of 1:1 at 37˚C in 5% CO_2 and saturated humidity, for 24, 48 and 72 h. PBS was used in place of BGC as a control.

Light and electron microscopy. MB49 cells were observed under an inverted microscope and by transmission electron microscopy, as previously described (18). Ultrathin sections were stained with 0.5% uranyl acetate and 0.04% lead citrate and observed under a transmission electron microscope JEM-2000EX (Jeol, Ltd., Tokyo, Japan) at 80 kV.

CCK-8 tumor cell viability assay. Cellular viability was assessed using a colorimetric cell counting kit, the Cell Counting Kit-8 (CCK-8; Dojindo, Japan), according to the manufacturer's instructions. MB49 cells ($1x10^5$ cells/well) were seeded in 96-well plates. At 90% confluency, *r*BCG, BCG, BCG+*h*IFN-α2b or PBS were added in triplicate to each well at an MOI of 10:1, and BCG (*r*BCG, BCG+*h*IFN-α2b) alone in medium was used as the blank control. CCK-8 solution (10 μl) was added to each well, and after 4 h the absorbance was read on a microplate reader at 450 nm. Cell growth inhibition rate (%) = $(1\text{-}Abs_{test}/Abs_{PBS})$ x 100%.

Apoptosis assay. Cells were seeded on coverslips in a 6-well plate, cultured in 3 ml RPMI-1640. When cells adhered, BCG or *r*BCG was added at an MOI of 1:1 and co-cultured for 24, 48 and 72 h. After 4% paraformaldehyde fixation, 10 μl of acridine orange (AO) (AppliChem, Gatersleben, Germany) dye mix (100 mg/l) was added to each well, and after 5 min, the slides were rinsed twice in PBS with 1% hydrochloric acid for 5 sec, then decolorized in $CaCl_2$ for 3-5 min. Staining with Hoechst 33258 (Sigma-Aldrich) was carried out according to the manufacturer's instructions, and the cells were observed under a fluorescence microscope (Nikon 80i; Nikon, Japan) (excitation 340 nm for Hoechst 33258, 502 nm for AO).

Cells grown in 6-well plates ($2x10^5$ cells/well) were incubated in the presence or absence of inducers, and then harvested by centrifugation at 4˚C and 1,000 x g for 5 min after trypsinization, and then rinsed twice with PBS. Cells were suspended in 100 μl binding buffer, and then stained in triplicate with the fluorescein isothiocyanate (FITC) Annexin V apoptosis detection kit (BD Biosciences, Bedford, MA, USA) at room temperature for 15 min. Thereafter, the flow cytometric analysis of cells was performed with BD FACSVantage SE cytometer (BD Biosciences) within 1 h.

FCM analysis of MHC-I expression. Cells were incubated with 5 μl FITC-anti-mouse MHC-I ($H\text{-}2K^b$) Ab (BD Biosciences) for 20 min. After washing with buffer [PBS containing 10 mmol/l ethylenediaminetetraacetic acid (EDTA) and 0.1% sodium azide], the cells were analyzed using the BD FACSVantage SE cytometer.

Murine orthotopic bladder cancer model and BCG treatment. We used a well-defined murine syngeneic orthotopic MB49 bladder cancer model to evaluate the role of rBCG *in vivo* (19). In brief, 6- to 8-week-old SPF female C57BL/6 mice (Animal

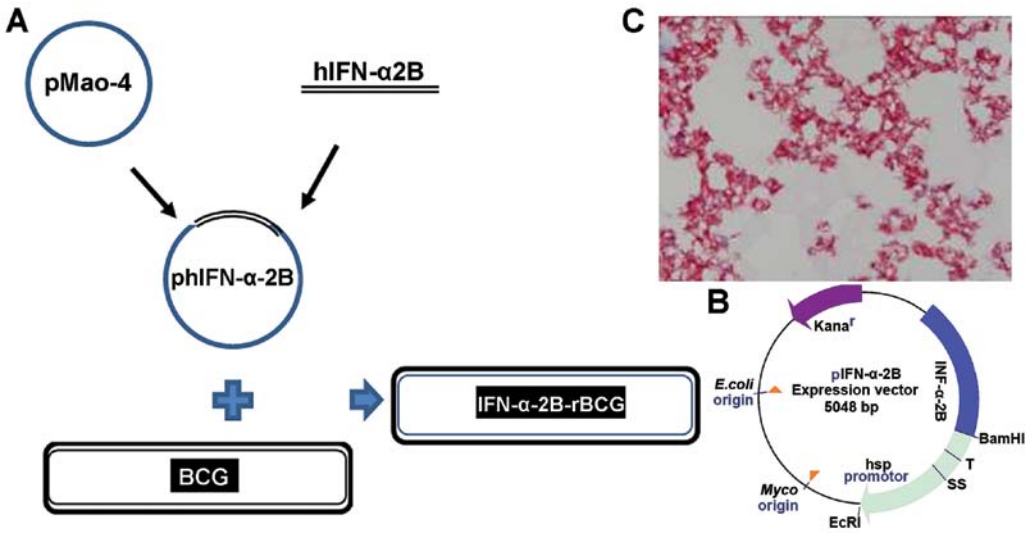

Figure 1. Construction strategy of recombinant human interferon-α-2b *Danish* 2 BCG. (A) Plasmid profile of shuttle expression vector, (B) *phIFN-α-2B*. The recombinant plasmid *phIFN-α-2B* was produced from the shuttle plasmid *pMAO-4* by cloning in the *h*IFN-α2b, enriched in DH5α-*E. coli* prior to extraction, and then electrically transduced into BCG. Four weeks after electrotransformation, *kanamycin* selection produced a single colony confirmed as *r*BCG by sequencing and positive acid-fast staining of classic *Mycobacterium* (C, oil immersion magnification, x1,000). BCG, Bacillus Calmette-Guérin; *r*BCG, recombinant *h*IFN-α2b-secreting BCG.

Laboratory Center, Beijing Medical University, China) upon approval by the Animal Use and Care Committee of Tianjin Medical University, were divided into 4 groups (n=15) and one group of controls (n=6). The 4 groups were catheterized to receive an intravesical inoculate of 10^5 MB49 bladder tumor cells on day 0 following a 5-sec treatment of the bladder wall with 30 µl of 0.2 M silver nitrite. On days 1, 8, 15 and 22 following tumor implantation, the mice were treated intravesically with 100 µl of either $3x10^8$ CFU/ml BCG, $3x10^8$ CFU/ml *r*BCG, $3x10^8$ CFU/ml BCG+*h*IFN-α2b or PBS. Exogenous *h*IFN-α2b was administered at the concentration achieved on day 7 of culture for the same amount of *r*BCG.

Survival was recorded daily for 6 weeks. Bladders were weighed to obtain the tumor growth inhibition rate (%) = (1 - $weight_{treated\ group}/weight_{control\ group}$) x 100%. Twelve hours after the last perfusion, blood was taken from 6 mice in each group through the inner canthus venous plexus.

Hematoxylin and eosin (H&E) and auramine O stainings. The bladder, liver, spleen, kidney, lung and heart of mice sacrificed on day 15 following the last perfusion and those that died during the observation period were immediately removed. Tissues were fixed in 4% paraformaldehyde, paraffin-embedded, and then H&E stained for pathological observation under a light microscope. For observation of mycobacteria in tissue, auramine O was applied for staining as follows. The paraffin section was dewaxed to water, dyed by auramine O solution for 5 min, decolorized with 3% hydrochloric acid alcohol for 1-2 min, then redyed 1-2 min in hematoxylin.

Immunohistochemistry. Mouse bladders were resected, shock frozen in liquid nitrogen and stored at -80˚C. Immunohistochemical staining of 5-Am cryostat sections with peroxidase-conjugated secondary antibodies was carried out as previously described (20) with mouse CD3, CD20 and Gr1; and mouse Fas (both from BD Biosciences, Heidelberg, Germany). The number of infiltrating immune cells, expressed as average number/high-power field (HP), was determined by examining 10 randomly selected non-overlapping microscopic fields at x400 magnification. To semi-quantify the cellular Fas expression, each slide was scored on the basis of percentage and intensity of stained tumor cells as previously described (21), as follows: no staining, 0; <20%, 1; 20-75%, 2; and >75%, 3. The intensity of staining was graded on the following scale: negative, 0; low, 1; moderate, 2; and strong, 3. The product of the scores for the intensity and positive rate of staining was the total score. In the present study, a final total score >2 for Fas expression was defined as high-expression. All cell counting results were verified between the manual and automated methods and are expressed as the viable cell numbers for interpretation. Scoring was carried out in a blinded manner by two independent individuals.

FCM analysis of T lymphocyte populations in peripheral blood. Whole blood samples were treated with EDTA, according to the manufacturer's instructions. Whole blood (100 µl) was incubated with directly conjugated fluorescent CD3/CD4/CD8 antibodies for 30 min in the dark at room temperature, and then red cells were lysed using FACS Lyse (both from BD Biosciences). Stained cells were washed and fixed in PBS with 1% formaldehyde, and samples were acquired on FACSVantage. Fluorescence minus one gating techniques were employed to establish staining thresholds and aid gating of T cell subpopulations.

Detection of cytokine secretion by ELISA. Heparinized whole blood supernatants (50 µl) were harvested, and *m*TNF-α and *m*IL-12 levels were assayed by ELISA (mouse TNF-α and IL-12 ELISA kit; Biosource, France) according to the manufacturer's instructions. The signal was detected using the BioTek Epoch microarray reader, and the results were analyzed using Gen5 software.

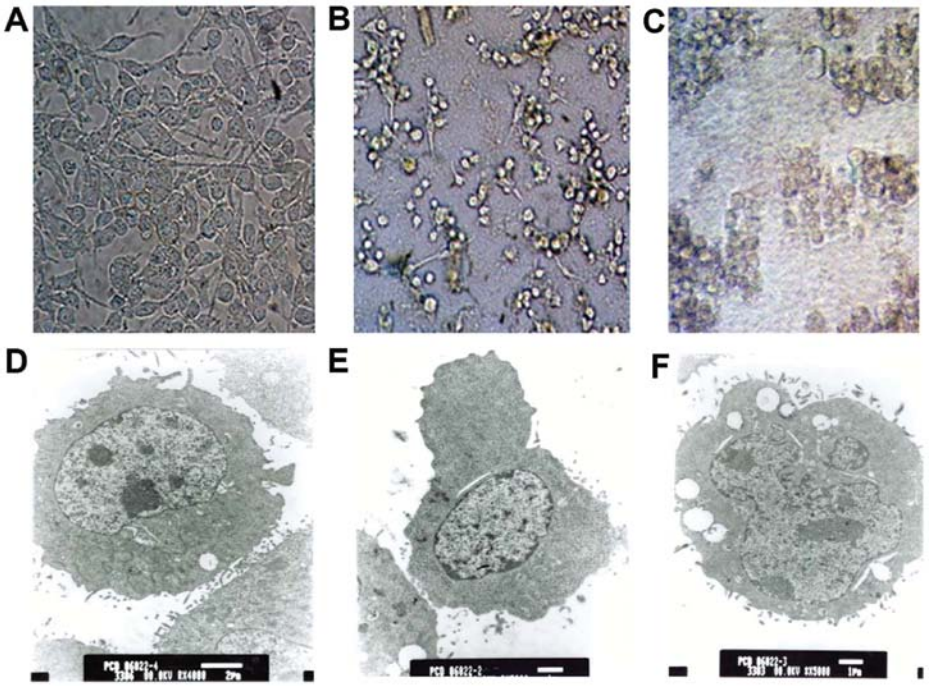

Figure 2. MB49 cell morphology: light microscope (scale bar, 50 μm, A-C; magnification, x200) and TEM (D-F). (A) Intact cells in the control group were generally bulky and wall-attached. (B) Cells treated with *r*BCG for 48 h shrunk, clumped and detached from the wall. (C) After 72 h, cellular morphology was abnormal and cell death was observed. (D) Intact cells contained ribosomes, mitochondria and endoplasmic reticulum in plasma, and protuberances and microvilli were present on the cell surface (scale bar, 2 μm; TEM magnification, x4,000). (E) After 48 h, the cell size was reduced, cytoplasm was condensed and bulges rather than microvilli were visible on the cell surface (scale bar, 1 μm; TEM magnification, x5,000). (F) After 72 h, irregular nuclei and large vacuoles were observed in the condensed cytoplasm (scale bar, 1 μm; TEM magnification, x5,000). TEM, transmission electron microscopy.

Statistical analyses. SPSS 18.0 software was used for data analysis. Results displayed represent the mean ± SD. One-way ANOVA followed by the Newman-Keuls *post-hoc* and Fisher exact test probability were used to compare values and rates between groups, respectively. ANOVA was employed for pairwise comparison of repeated measurements. Survival of the mice was evaluated using Kaplan-Meier plots and the log-rank test. Statistical analyses are given as two-sided p-values. $p<0.05$ was considered to indicate a statistically significant result, and $p<0.01$ indicated extreme significance.

Results

rBCG affects bladder cancer cell morphology. Untreated MB49 cells were mostly round or of irregular shape, began to adhere to the well wall after 1-2 h culture, and extended cytoplasmic protrusions were observed after 12 h. MB49 cells demonstrated a high nuclear/cytoplasmic ratio, uneven chromatin and the mitotic phase was occasionally observed (Fig. 2A and D).

During co-culture with BCG, *r*BCG or BCG+*h*IFN-α2b cellular refraction decreased, cytoplasmic protrusions gradually disappeared, soma became stubby and the cytoplasm became granular (Fig. 2B and E). After 48 h, the cells had clearly shrunk, protuberances disappeared, cells rounded up and proliferation slowed (Fig. 2B and E). Some cells grew in suspension and formed clumps surrounded by bacteria. After 72 h, the cells were granular, sparsely distributed, and some exhibited vacuolization, blebbing and lytic necrosis (Fig. 2C and F). The less damaged cells showed mitochondrial swelling, large vacuolar degeneration, dissolved nuclear chromatin, cytoplasm necrosis and surface microvilli decrement (Fig. 2F).

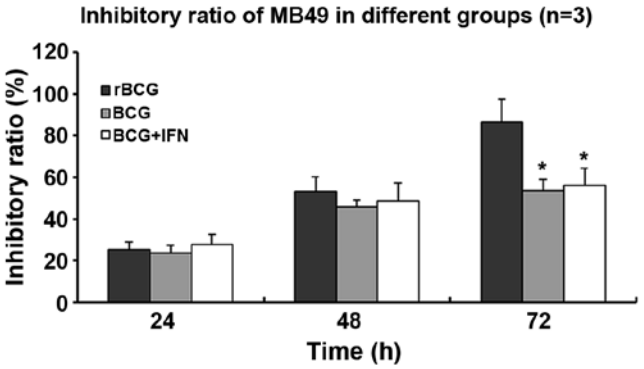

Figure 3. Growth inhibitory ratio of MB49 cells incubated with BCG, *r*BCG or BCG+IFN. MB49 cells were seeded at an initial density of $1x10^6$ cells/ml, and incubated for 24, 48 and 72 h with an MOI of 10:1 BCG and/or BCG+IFN. The inhibitory ratio was determined by CCK-8. $^*p<0.05$ vs. *r*BCG at 72 h.

rBCG inhibits tumor cell growth and induces apoptosis. MB49 cells incubated with *r*BCG grew less quickly than the controls incubated with PBS (Fig. 3). After 72 h, *r*BCG achieved a significantly higher inhibitory ratio (86.37±3.67%) than BGC (53.43±1.84%) or BCG+*h*IFN-α2b (56.03±2.79%) (all $p<0.05$) (Fig. 3).

Intact MB49 cells stained with AO adhered and grew vigorously. The nuclei emitted yellow or green fluores-

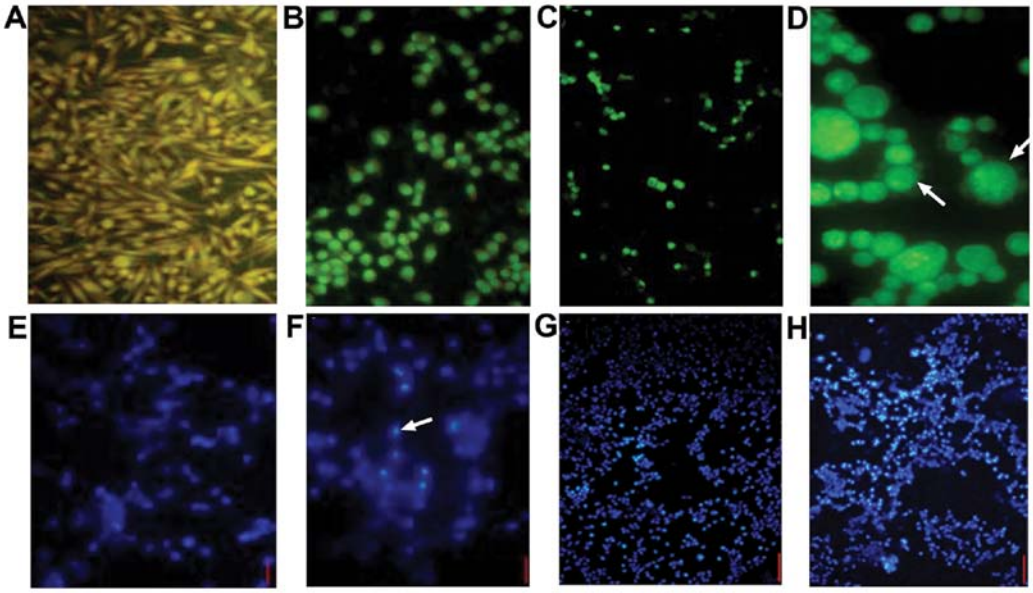

Figure 4. Fluorescence imaging of bladder tumor cells stained with (A-D) AO and (E-H) Hoechst 33258. (A) Intact MB49 cells were spindle-shaped and nuclei fluoresced yellow/green and the cytoplasm emitted orange/red fluorescence, indicating a high karyoplasmic ratio (FSM, x100). (B) After 48 h in the presence of *r*BCG, the cells became rounded and clumped, cytoplasmic protuberances disappeared, the karyoplasmic ratio increased and vesicular bulging membrane and apoptotic bodies were observed (FSM, x200), (C) After 72 h, significantly fewer cells were observed (FSM, x100). (D) Apoptotic cells forming typical petal-like structures (FSM, x400). (E) Intact cells showed faint blue luminescence under UV (FSM, x200). (F) Luminous apoptotic bodies were observed (FSM, x200). (G and H) Cells incubated with *r*BCG for 48 and 72 h (FSM, x40).

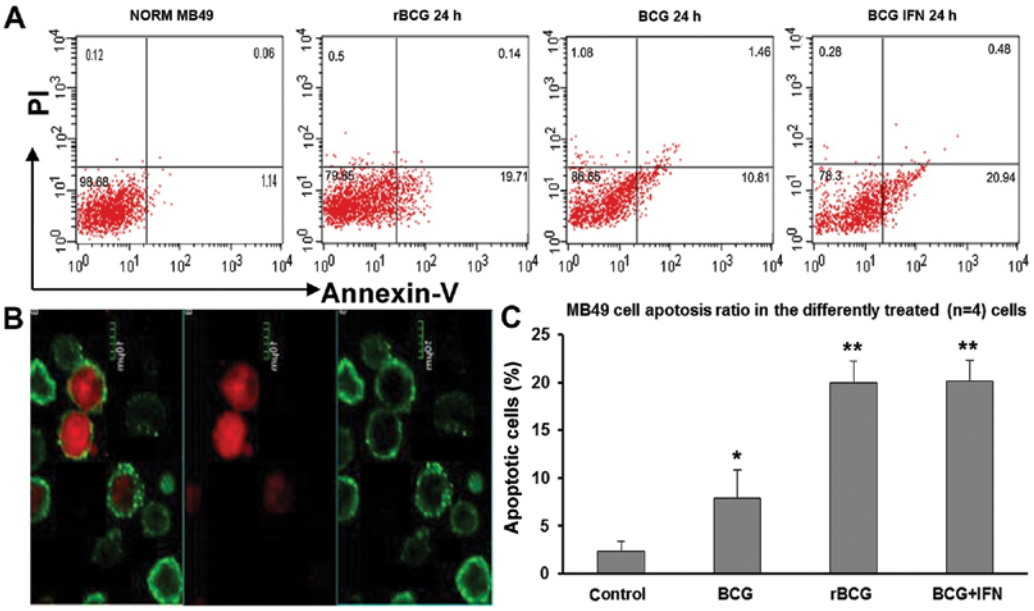

Figure 5. MB49 cell apoptosis. (A) Representative images of Annexin V/PI staining of MB49 cells incubated alone or with BCG, *r*BCG or *r*BCG+IFN. The upper right quadrant (PI^+/Annexin V^+) displays dead and late apoptotic cells, the left lower quadrant displays living cells (PI^-/Annexin V^-), the lower right quadrant (PI^-/Annexin V^+) displays early apoptotic cells. (B) MB49 cell apoptosis and death were detected by confocal laser scanning microscopy. Dead cells were stained internally with PI and apoptotic cell membranes were stained with Annexin V (magnification, x400). (C) Flow cytometry showing MB49 cell apoptosis in the control, BCG, *r*BCG and BCG+IFN groups. Data are shown as the mean ± SD. n=4; $^*p<0.05$; $^{**}p<0.01$ vs. control group.

cence, and the cytoplasm emitted orange red fluorescence, indicating a high karyoplasmic ratio and cells were spindle shaped (Fig. 4A). MB49 cells incubated for 24 h with *r*BCG, BCG or BCG+*h*IFN-α2b were not obviously affected, yet after 48 h, the cells clumped, cytoplasmic protuberances gradually disappeared, the karyoplasmic ratio decreased, and vesicular bulging membranes and apoptotic bodies were observed (Fig. 4B). After 72 h, the cells no longer adhered firmly, and the cell number and karyoplasmic ratio were reduced (Fig. 4C and D). Hoechst 33258 staining revealed apoptotic bodies at 48 and 72 h (Fig. 4E-H).

The rate of apoptosis was 2.31±1.02% in the control cells, but after 24 h the presence of BGC, *r*BCG and BCG+*h*IFN-α2b significantly increased the rate of apoptosis to 7.9±0.97%

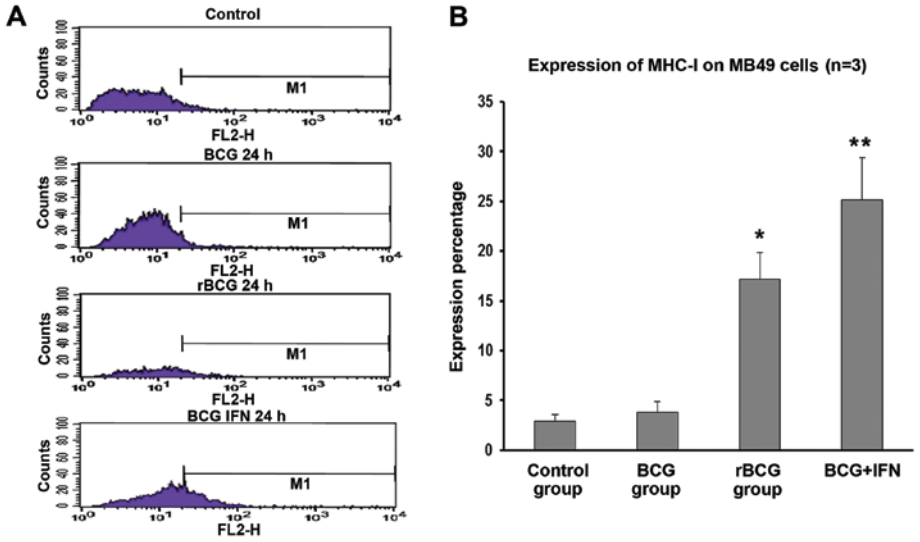

Figure 6. MHC-I expression on tumor cells detected by FCM. (A) Representative images of MHC-I expression in control cells, and cells incubated with BCG, *r*BCG or *r*BCG+*h*IFN-α2b for 24 h. (B) Comparison of MHC-I expression in control cells, and cells incubated with BCG, *r*BCG or *r*BCG+IFN for 24 h (mean ± SD). n=3; *p<0.05; **p<0.01 vs. control group. FCM, flow cytometry.

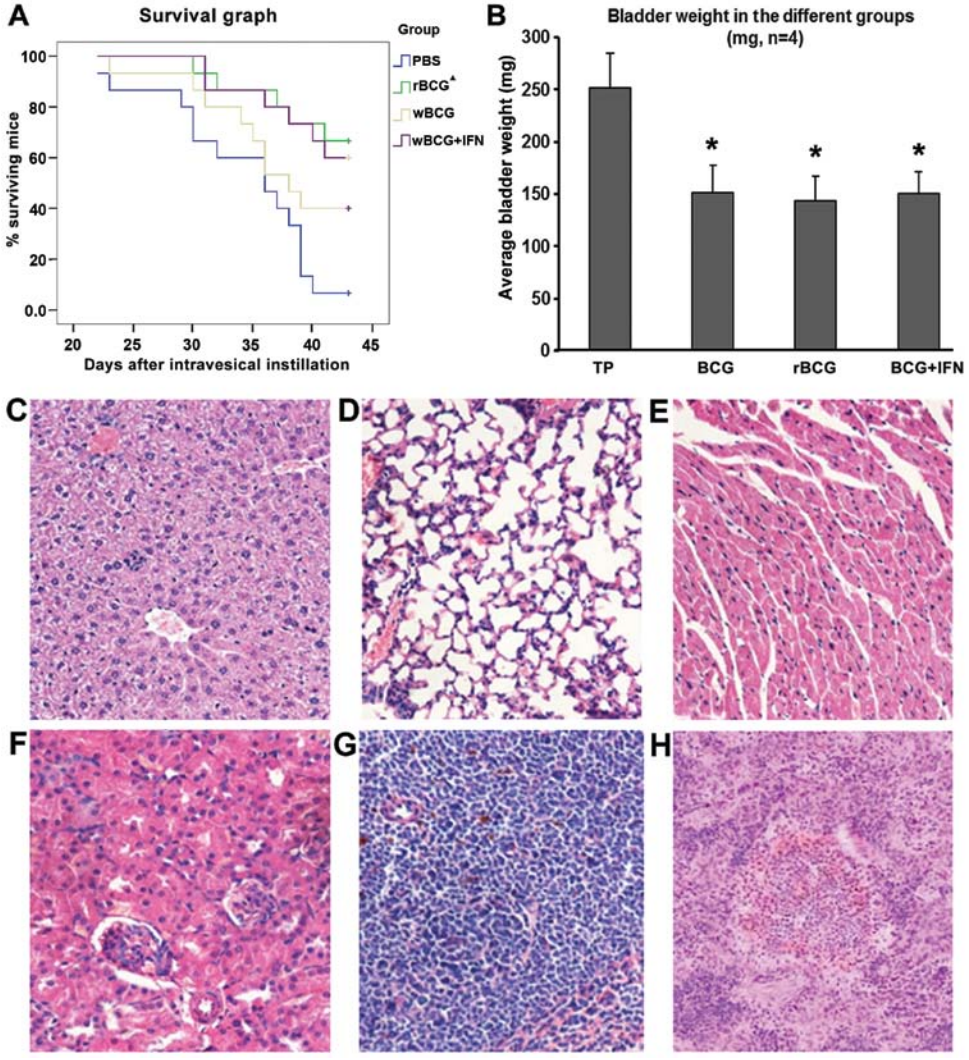

Figure 7. Tumor growth and survival in the C57BL/6 mice and microscopic morphology of the organ tissues. (A) Survival of mice following tumor establishment. Black triangles indicate that the survival of mice administered *r*BCG was higher than mice administered BCG (p<0.05), and did not differ significantly from the mice administered BCG+IFN. (B) Average bladder weight (mean ± SD, n=4). *p<0.001 vs. the TP group. TP group, tumor-bearing mice administered PBS. (C) Liver, (D) lung, (E) heart, (F) kidney and (G) spleen of the tumor-bearing mice administered *r*BCG all showed no obvious abnormal, no tumor metastasis and miliary pattern. (H) Individual mouse spleen showed hyperplasia (H, magnification, x100; C-G, magnification, x200).

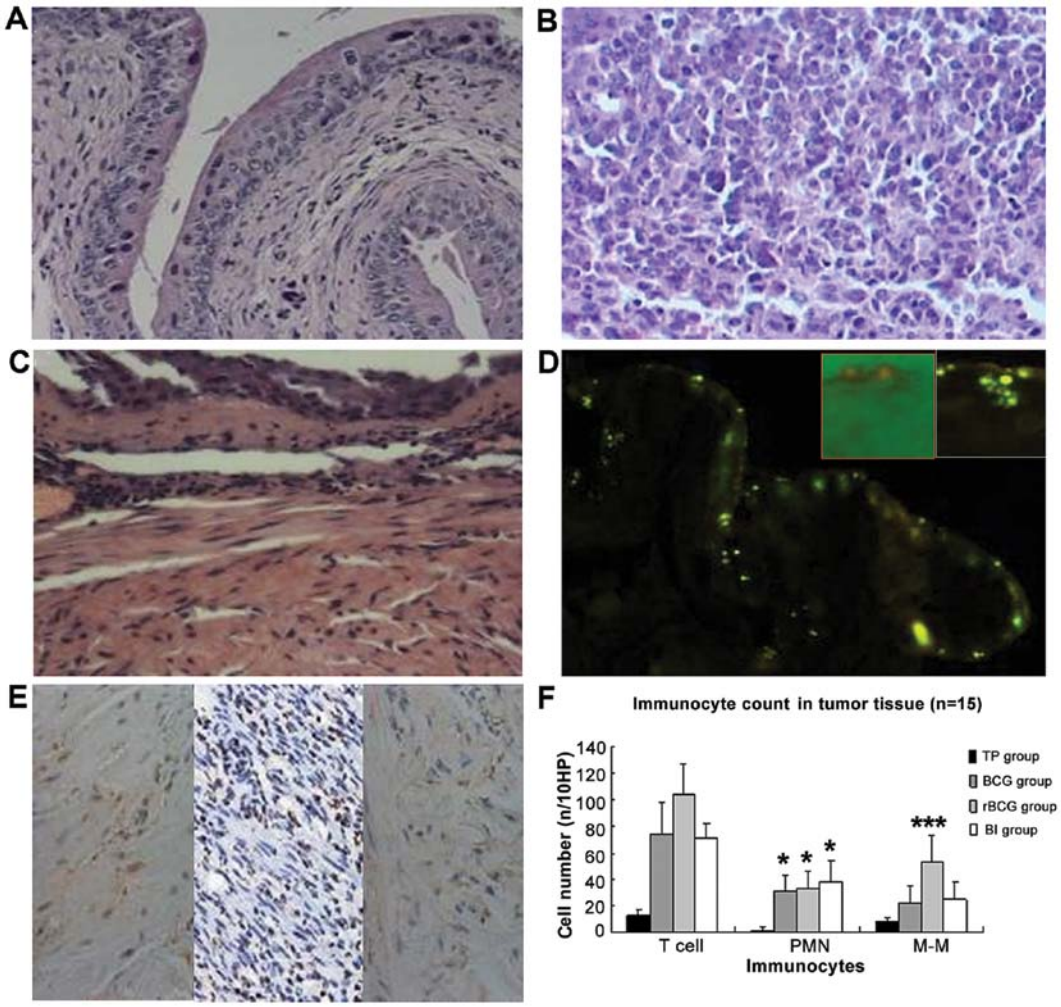

Figure 8. H&E staining and immunocyte content of the bladder and cancer tissues in the C57BL/6 mice (A-C, magnification, x200; F, magnification, x100). (A) Untreated bladder exhibited normal morphology. (B) Tumor tissue formed by seeded MB49 cells did not affect normal bladder structure; tumor cells were diffusely infiltrated. (C) After BCG administration, submucosal edema appeared, vasodilation was evident and inflammatory cells infiltrated the submucosal layer. (D) After 24 h of BCG administration, auramine O-positive bacteria were detected within and underlying the urothelial cells. The red frame is the merge of the bright and fluorescent field 2 h after BCG administration, indicating BCG adhesion to the intimal. The white frame displays BCG taken up by the epithelium. (E) IHC image of CD20, CD3 and Gr1 staining in the *r*BCG-treated bladder (magnification, x400). (F) Comparison of immunocyte content in the tumor tissues. Data are shown as means ± SD (n/10 HP). *p<0.05; ***p<0.001 vs. the TP group. TP group, tumor-bearing mice administered PBS; BI group, BCG+IFN group. H&E, hematoxylin and eosin. PMN, polymorphonuclear leukocytes; M-M, monocytes/macrophages.

(p<0.05), 19.92±0.77% (p<0.01) and 20.11±0.74% (p<0.01), respectively (Fig. 5).

rBCG promotes MHC-I expression on MB49 cells. MB49 cells were incubated with MHC-I-directed antibody and staining was detected by flow cytometry. A 24-h incubation with BCG did not significantly influence the fraction of MHC-I^{+} cells (2.89±0.24%). However, *r*BCG and BCG+*h*IFN-α2b increased the fraction of MHC-I^{+} cells to 17.18±0.88% (p<0.05) and 25.13±1.42% (p<0.01), respectively (Fig. 6).

rBCG inhibits tumor growth and promotes survival in a mouse model of orthotopic bladder cancer. After 2 weeks of modeling, C57BL/6 mice exhibited different degrees of hematuria. After 6 weeks, several mice developed a hypogastric mass of 0.5-2 cm upon palpation. Mice administered *r*BCG (n=5) survived for significantly longer than mice administered BCG (n=7) (p<0.001), yet did not survive significantly longer than mice administered BCG+*h*IFN-α2b (n=8) (Fig. 7A).

The average bladder weight was significantly lower in mice administered *r*BCG (143.6±1.6 mg) than that in mice administered PBS (n=14) (251.5±2.2 mg, p<0.001, Fig. 7B). Average bladder weight was reduced by 39.9% in mice administered BCG, 42.9% in mice administered rBCG and 40.2% in mice administered BCG+*h*IFN-α2b.

The bladder, liver, spleen, kidney, lung and heart of the mice sacrificed following the last perfusion and those that died during the observation period indicated no tumor metastasis and miliary nodules. No significant difference in pathological features was observed among the mice treated with BCG, *r*BCG or BCG+*h*IFN-α2b (Fig. 7C-H).

rBCG induces immunity in the bladder. The pathological morphology of the bladder tissue indicated diffuse infiltration of tumor cells with high-grade malignancy (Fig. 8A and B). Administration of BCG, *r*BCG and BCG+*h*IFN-α2b induced bladder inflammation. Migrating inflammatory cells were observed in the submucosa. The local inflammatory reaction

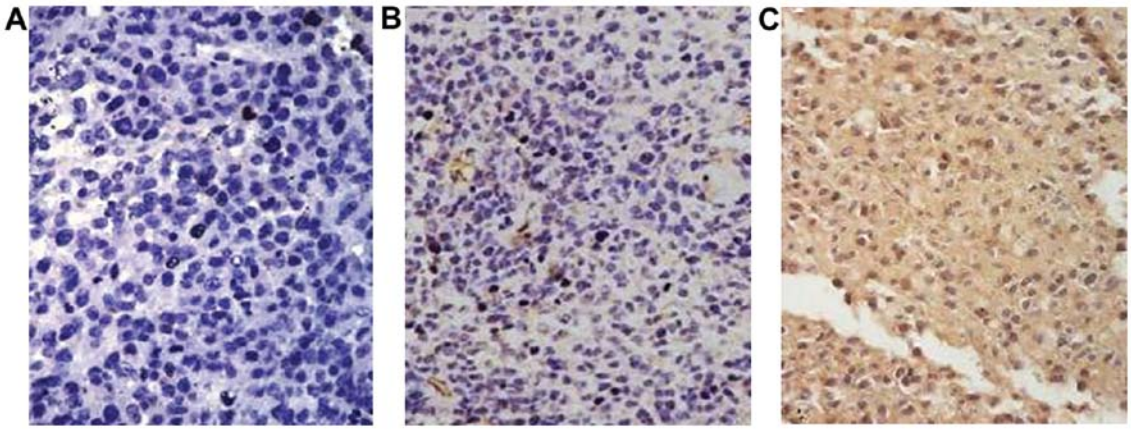

Figure 9. Fas immunohistochemical staining in the C57BL/6 mouse bladder cancer tissues. Fas was detected only in the cytoplasm of the cells. (A) Fas-negative tissue showed cytoplasm and cell membrane stained blue or light blue. (B and C) Positive staining was indicated by brown uniform fine particles located in the cytoplasm and on the cell membrane. (A) Negative control (isotype-matched control; magnification, x200). (B) Mouse bladder tumors had low Fas expression (magnification, x100). (C) The tumor tissue treated by BCG showed positive expression of Fas (magnification, x100).

Table I. Fas expression in the tumors (cases) according to the IHC results.

Groups	Low expression	High expression
TP	14	1
BCG[a]	4	11
*r*BCG[a]	1	13
BI[a]	4	10

[a]p<0.001 vs. TP group. C57BL/6 mice were administered BCG, *r*BCG and *r*BCG+IFN, as presented in Fig. 7.

in response to BCG was characterized by an initial increase in blood flow, enhanced vascular permeability characterized by edema, and an influx of effector cells. Vasodilation was evident and leukocytes populated the submucosal layer (Fig. 8C). After administration of BCG into the mouse bladder, auramine O staining-positive bacteria were detected within and underlying urothelial cells, indicating that BCG was taken up by the epithelium (Fig. 8D).

Immunohistochemical staining indicated infiltration of $CD3^+$ lymphocytes, $CD20^+$ monocytes and Grl^+ polymorphonuclear leukocytes (PMNs) (Fig. 8E and F). PMN, monocyte and T lymphocyte infiltration increased significantly in the treated groups, compared with the infiltration in the control group (all $p \leq 0.05$). Monocyte and T cell counts were significantly higher in mice administered rBCG than these counts in the mice administered BCG or BCG+*h*IFN-α2b (both p=0.000). However, PMN counts did not differ significantly between the treated animals.

rBCG increases the expression of Fas. Fas expression was initially low in the bladder tumor tissues. Administration of BCG, *r*BCG and BCG+*h*IFN-α2b significantly increased Fas expression (p=0.000), but the intensity of Fas staining did not differ significantly between the three treated groups (Fig. 9 and Table I).

rBCG increases the ratio of $CD4^+$/$CD8^+$ in peripheral blood. In comparison to normal mice, the tumor-bearing mice had depressed levels of peripheral blood $CD4^+$ cells and lower $CD4^+$/$CD8^+$ ratios. However, administration of BCG, *r*BCG or BCG+*h*IFN-α2b elevated $CD4^+$ cell counts and $CD4^+$/$CD8^+$ ratios to near-normal levels (Fig. 10A-C) (all p<0.01). However, no significant difference in these values was detected between the three treatment groups.

rBCG increases the level of TNF-a and IL-12. *r*BCG administration increased circulating levels of *m*TNF-α and *m*IL-12 to 02.33±11.00 and 854.46±4.56 pg/ml, respectively (Fig. 10D). However the circulating levels of these cytokines did not differ significantly among mice administered rBCG, BCG or BCG+*h*IFN-α2b.

Discussion

BCG prevents bladder cancer-related metastasis and decreases bladder cancer-associated mortality. Although systemic reactions have been reported, the likely mechanism of BCG action involves local inflammation (1). We sought to further characterize the mechanism of action of BCG in a bladder cancer cell line and an orthotopic murine bladder cancer model.

Due to the involvement of the host immune system in BCG efficacy, immunodeficient mice are not suitable for investigation of its mechanism of action. We instead established an orthotopic bladder tumor model in which the mouse bladder tumor cell line MB49 was implanted into the C57BL/6 mouse bladder. C57BL/6 mice were chosen, as they are widely used, permitting direct comparison with previously established clinical baselines (22). Following chemical injury and cell transplantation (19), tumor cell proliferation was observed, yet no tumor metastasis and miliary nodules were found in all groups.

A wide range of *r*BCG vaccine candidates expressing bacterial, viral, parasitic antigens have previously been developed, and *r*BCG strains secreting mouse and human cytokines, primarily Th1 cytokines (e.g., IL-2, IL-18, IFN-γ and IFN-α),

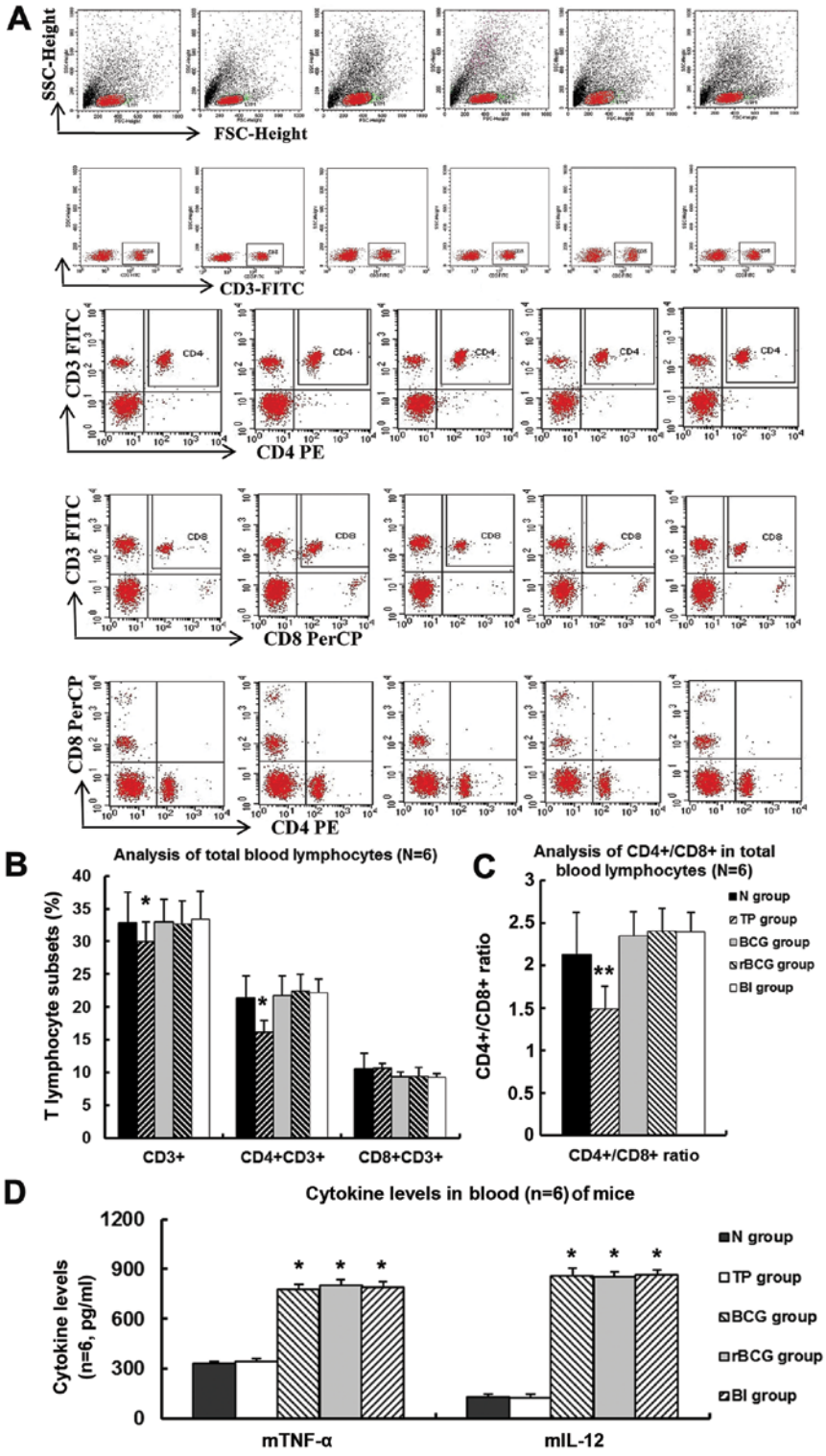

Figure 10. T lymphocyte subsets and cytokines in peripheral blood of C57BL/6 mice administered BCG, *r*BCG or BCG+IFN as analyzed by FCM. (A) Representative images of $CD3^+$, $CD3^+CD8^+$ and $CD3^+CD8^+$ lymphocytes in the peripheral blood of mice administered BCG, *r*BCG or BCG+IFN, and (B) the percentage of $CD3^+$, $CD3^+CD8^+$ and $CD3^+CD8^+$ lymphocytes in the peripheral blood of mice administered BCG, *r*BCG or BCG+IFN (mean ± SD) (n=6). $^*p<0.05$ vs. normal. (C) $CD4^+/CD8^+$ ratio, mean ± SD (n=6). $^{**}p<0.01$ vs. normal. (D) The level of *m*TNF-α and *m*IL-12 in the peripheral blood of the C57BL/6 mice administered BCG, *r*BCG or BCG+IFN, mean ± SD (n=6, pg/ml). $^*p<0.001$ vs. normal. N, normal group; TP group, tumor-bearing mice administered PBS; BI group, BCG+IFN group

have previously been investigated (10). We studied the influence of *h*IFN-*α*2b-*r*BCG on tumor growth *in vitro* and both tumor growth and the systemic and local immune response *in vivo*. We used the BCG *Shanghai* substrain, derived from the *Danish* 2 strain that has been used for tuberculosis prevention and immune-modulation universally in China. We engineered a strain of BCG *Danish* 2 to secrete high levels of recombinant *h*IFN-*α*2b.

Direct effects on tumor cells. We found that both BCG and rBCG inhibited growth of a mouse bladder cancer cell line, inducing morphological changes and apoptosis, while *r*BCG was significantly more potent. IFN induces tumor cell apoptosis by promoting protooncogenes and TNF-α receptor expression, or by inhibiting intracellular proteins (23,24). Following administration to mice, we observed BCG adherence to the bladder intima prior to bladder pathologic changes, a process that has previously been reported to involve non-specific, physicochemical and specific receptor-ligand-mediated events (7,25). Phospholipids, lipids, wax D, bacterial proteins and lipopolysaccharides in BCG are all strongly immunogenic (26-28), and BCG cell wall protein and Arabian-polysaccharide pathogen-associated molecular patterns induce expression of lysosomal membrane protein and apoptosis in host cells (27-29). A BCG cell wall glycolipid, trehalose dimycolate, has also been reported to damage host cells by attacking the mitochondrial membrane, affecting cellular respiration and energy metabolism, destroying microsomal enzymes and inducing programmed cell death (30-33). Furthermore, internalized BCG increased production of intracellular cytotoxic nitric oxide, which at a high concentration, causes DNA damage, and cytostatic and cytotoxic effects (7). BCG has also been reported to induce upregulation of certain surface molecules and cytokines in epithelial cells (34,35), and activation of the signal transduction pathways involving activator protein 1 and NFκB (36,37).

We also observed cytoplasmic Fas in mouse bladder tumor cells, and administration of *r*BCG and BCG upregulated Fas expression on the surface of the tumor cells. Fas typically is highly expressed in rapidly proliferating cells and injured tissues, and the triggering of Fas by its ligand induces apoptosis in target cells (38). Expression of Fas can be upregulated by IL-2 and IFNs (39), but we observed no significant difference between Fas expression in the *r*BCG- and BCG-treated cells, potentially due to the species specificity of human IFN.

Immunomodulation. BGC has been hypothesized to ameliorate the aberrant imbalance of T helper and cytotoxic T cell subsets observed in the bladder during proliferation of cancer cells (3). Systemic immunity is induced by administration of BGC in patients with bladder cancer and a cytokine profile typical of active tuberculosis can be observed (40). In our mouse model, the circulating levels of $CD3^+$ and $CD4^+$ cells, and the $CD4^+/CD8^+$ ratio was lower in the tumor-bearing mice than in the normal animals. This immune response was likely caused by activation and proliferation of antigen-specific T lymphocytes, followed by immune tolerance or apoptosis, and depletion of T lymphocytes by activation-induced cell death. Administration of both BCG and *r*BCG induced lymphocyte proliferation, and regulated lymphocyte subsets, adjusting cellular immune function. $CD4^+$ and $CD3^+$ cell counts recovered to the levels observed in healthy control animals, yet the level of $CD8^+$ cells was not significantly influenced. The $CD4^+/CD8^+$ ratio was also increased, but no significant difference was observed between the effect of BCG and *r*BCG.

Local immune responses. A small number of local lymphocytes are usually observed in the tumor tissue of patients with bladder tumors, mainly distributed in the submucosa (41). Administration of BCG in our mouse model of bladder cancer caused extensive local inflammation in the bladder wall. Expression of CD3, CD20 and Gr1 in the tumors was negative or weak, yet administration of BCG or rBCG induced influx of PMNs and other inflammatory cells. BCG appears to activate local non-specific Th1 type cells and cytokines (42). We observed that BCG and *r*BCG induced acute inflammation of the bladder, characterized by a strong vascular component and edema, followed by a gradual influx of monocytes/macrophages, T lymphocytes and NK cells, which form chronic granuloma-like cellular infiltrates in the suburothelial stroma (3).

In vitro, BCG also induced MHC-I expression on mouse MB49 cells, as previously reported by Shankaran *et al* (43), and we found that *r*BCG did so more potently than BCG. Tumor cells often downregulate MHC-I to avoid immune surveillance (44), yet IFN is well known to induce MHC-I (45). Increased expression of MHC-I on the tumor cell surface likely enhances the immunogenicity of these cells.

Cytokine release. Patients with bladder tumors often exhibit a marked polarization towards expression of Th2 type cytokines while expression of Th1 cytokines are suppressed (46). Administration of BCG adjusted the imbalance of Th1 cytokines (IL-2, IL-12, IFN-γ and TNF-α) leading to detection of these cytokines in the urine of BCG-treated patients (7). The induction of proinflammatory cytokines, specifically IFN-γ, TNF-α and IL-2, are crucial for the cytotoxic effect of live BCG-activated cells (47). BCG-activated lymphocytes and macrophages are the most likely sources of these cytokines, but at present, other cellular sources such as urothelial cells cannot be ruled out (7,46). We found that administration of BCG and *r*BCG promoted Th1 type immunity in the tumor-bearing mice. *In vitro,* IFN-α*2b* enhances the BCG induction of Th1 immune responses in human PBMCs (48), yet this effect was not observed in the peripheral blood of our experimental animals. T cell-mediated cell lysis and release of regulatory cytokines have been shown to represent late acquired immune events of the antitumor effector phase (49), to induce tumor apoptosis and prevent tumor growth. For example, IL-12 promotes the activation of effector cells and induces IFN-γ, IL-2 and TNF-α (50). TNF-α kills tumor cells directly and also induces apoptosis by the Fas/FasL-mediated path or others, which all could be strengthened by IFN.

In conclusion, our findings suggest that the therapeutic effects of BCG can be attributed in part to the rapid accumulation of antigen-presenting, and activated immune cells responsible for the production of a multiphasic immune response as demonstrated by the presence of the Th1 or Th2 phenotype. IFN directly inhibits proliferation and angiogenesis (51), and further immunomodulation of tumor MHC expression (52), could be advantageous in bladder cancer treatment. According to our results *r*BCG also exhibited antitumor activity in the bladder of mice transplanted with a bladder cancer cell line. Mice administered *r*BCG survived longer than those administered BCG plus endogenous IFN. Although the capacity of *r*BCG to inhibit tumor growth was not superior to that of BCG, the influence of the secreted cytokine may have been limited by species specificity. As a novel

immune-modulatory agent for the treatment of human bladder cancer, *r*BCG has excellent prospects for development, but more in-depth exploration of its function and mechanisms is needed.

Acknowledgements

The present study was supported by the National Natural Science Foundation of China (no. 81402095). We thank Professor M.A. O'Donnell and Professor Yi Luo for kindly providing plasmid *pMAO-4* to construct the recombinant *h*IFN-α2b-secreting BCG.

References

1. Gandhi NM, Morales A and Lamm DL: Bacillus Calmette-Guérin immunotherapy for genitourinary cancer. BJU Int 112: 288-297, 2013.
2. Hall MC, Chang SS, Dalbagni G, Pruthi RS, Seigne JD, Skinner EC, Wolf JS Jr and Schellhammer PF: Guideline for the management of nonmuscle invasive bladder cancer (stages Ta, T1, and Tis): 2007 update. J Urol 178: 2314-2330, 2007.
3. Alexandroff AB, Nicholson S, Patel PM and Jackson AM: Recent advances in bacillus Calmette-Guerin immunotherapy in bladder cancer. Immunotherapy 2: 551-560, 2010.
4. Haley JL, Young DG, Alexandroff A, James K and Jackson AM: Enhancing the immunotherapeutic potential of mycobacteria by transfection with tumour necrosis factor-alpha. Immunology 96: 114-121, 1999.
5. Ratliff TL, Kavoussi LR and Catalona WJ: Role of fibronectin in intravesical BCG therapy for superficial bladder cancer. J Urol 139: 410-414, 1988.
6. Kresowik TP and Griffith TS: Bacillus Calmette-Guerin immunotherapy for urothelial carcinoma of the bladder. Immunotherapy 1: 281-288, 2009.
7. Bevers RF, Kurth KH and Schamhart DH: Role of urothelial cells in BCG immunotherapy for superficial bladder cancer. Br J Cancer 91: 607-612, 2004.
8. Williams SK, Hoenig DM, Ghavamian R and Soloway M: Intravesical therapy for bladder cancer. Expert Opin Pharmacother 11: 947-958, 2010.
9. Delimpoura V, Samitas K, Vamvakaris I, Zervas E and Gaga M: Concurrent granulomatous hepatitis, pneumonitis and sepsis as a complication of intravesical BCG immunotherapy. BMJ Case Rep 10: 2013, 2013.
10. Kawai K, Miyazaki J, Joraku A, Nishiyama H and Akaza H: Bacillus Calmette-Guerin (BCG) immunotherapy for bladder cancer: Current understanding and perspectives on engineered BCG vaccine. Cancer Sci 104: 22-27, 2013.
11. Joudi FN, Smith BJ, O'Donnell MA; National BCG-Interferon Phase 2 Investigator Group: Final results from a national multicenter phase II trial of combination bacillus Calmette-Guérin plus interferon alpha-2B for reducing recurrence of superficial bladder cancer. Urol Oncol 24: 344-348, 2006.
12. Nepple KG, Lightfoot AJ, Rosevear HM, O'Donnell MA, Lamm DL; Bladder Cancer Genitourinary Oncology Study Group: Bacillus Calmette-Guérin with or without interferon α-2b and megadose versus recommended daily allowance vitamins during induction and maintenance intravesical treatment of nonmuscle invasive bladder cancer. J Urol 184: 1915-1919, 2010.
13. Lam JS, Benson MC, O'Donnell MA, Sawczuk A, Gavazzi A, Wechsler MH and Sawczuk IS: Bacillus Calmete-Guérin plus interferon-alpha2B intravesical therapy maintains an extended treatment plan for superficial bladder cancer with minimal toxicity. Urol Oncol 21: 354-360, 2003.
14. Bazarbashi S, Soudy H, Abdelsalam M, Al-Jubran A, Akhtar S, Memon M, Aslam M, Kattan S and Shoukri M: Co-administration of intravesical bacillus Calmette-Guérin and interferon α-2B as first line in treating superficial transitional cell carcinoma of the urinary bladder. BJU Int 108: 1115-1118, 2011.
15. Askeland EJ, Newton MR, O'Donnell MA and Luo Y: Bladder cancer immunotherapy: BCG and beyond. Adv Urol 2012: 181987, 2012.
16. Chapman R, Chege G, Shephard E, Stutz H and Williamson AL: Recombinant *Mycobacterium bovis* BCG as an HIV vaccine vector. Curr HIV Res 8: 282-298, 2010.
17. Sun E, Nian X, Liu C, Fan X and Han R: Construction of recombinant human IFNa-2b BCG and its antitumor effects on bladder cancer cells in vitro. Genet Mol Res 14: 3436-3449, 2015.
18. Mugabe C, Raven PA, Fazli L, Baker JH, Jackson JK, Liggins RT, So AI, Gleave ME, Minchinton AI, Brooks DE, *et al*: Tissue uptake of docetaxel loaded hydrophobically derivatized hyperbranched polyglycerols and their effects on the morphology of the bladder urothelium. Biomaterials 33: 692-703, 2012.
19. Luo Y, Chen X and O'donnell MA: Use of prostate specific antigen to measure bladder tumor growth in a mouse orthotopic model. J Urol 172: 2414-2420, 2004.
20. Bayne LJ and Vonderheide RH: Immunohistochemical assessment of immune cells in mouse tumor tissue. Cold Spring Harb Protoc 2013: 843-848, 2013.
21. Ohuchida K, Mizumoto K, Ishikawa N, Fujii K, Konomi H, Nagai E, Yamaguchi K, Tsuneyoshi M and Tanaka M: The role of S100A6 in pancreatic cancer development and its clinical implication as a diagnostic marker and therapeutic target. Clin Cancer Res 11: 7785-7793, 2005.
22. Saban MR, Simpson C, Davis C, Wallis G, Knowlton N, Frank MB, Centola M, Gallucci RM and Saban R: Discriminators of mouse bladder response to intravesical Bacillus Calmette-Guerin (BCG). BMC Immunol 8: 6, 2007.
23. Yanase N, Hayashida M, Kanetaka-Naka Y, Hoshika A and Mizuguchi J: PKC-δ mediates interferon-α-induced apoptosis through c-Jun NH_2-terminal kinase activation. BMC Cell Biol 13: 7, 2012.
24. Yanase N, Kanetaka Y and Mizuguchi J: Interferon-α-induced apoptosis via tumor necrosis factor-related apoptosis-inducing ligand (TRAIL)-dependent and -independent manner. Oncol Rep 18: 1031-1038, 2007.
25. Chen F, Zhang G, Iwamoto Y and See WA: Bacillus Calmette-Guerin initiates intracellular signaling in a transitional carcinoma cell line by cross-linking alpha 5 beta 1 integrin. J Urol 170: 605-610, 2003.
26. Villeneuve C, Gilleron M, Maridonneau-Parini I, Daffé M, Astarie-Dequeker C and Etienne G: Mycobacteria use their surface-exposed glycolipids to infect human macrophages through a receptor-dependent process. J Lipid Res 46: 475-483, 2005.
27. Moriwaki Y, Begum NA, Kobayashi M, Matsumoto M, Toyoshima K and Seya T: *Mycobacterium bovis* Bacillus Calmette-Guerin and its cell wall complex induce a novel lysosomal membrane protein, SIMPLE, that bridges the missing link between lipopolysaccharide and p53-inducible gene, *LITAF(PIG7)*, and estrogen-inducible gene, *EET-1*. J Biol Chem 276: 23065-23076, 2001.
28. Kato T, Bilim V, Yuuki K, Naito S, Yamanobe T, Nagaoka A, Yano I, Akaza H and Tomita Y: Bacillus Calmette-Guerin and BCG cell wall skeleton suppressed viability of bladder cancer cells in vitro. Anticancer Res 30: 4089-4096, 2010.
29. Ishibashi T, Yamada H, Harada S, Harada Y, Takamoto M and Sugiyama K: Comparison of the mode of immunopotentiating action of BCG and wax D. II. Effect on the methylcholanthrene carcinogenesis. Jpn J Exp Med 47: 435-440, 1977.
30. Kato M: Action of a toxic glycolipid of *Corynebacterium diphtheriae* on mitochondrial structure and function. J Bacteriol 101: 709-716, 1970.
31. Fujita Y, Okamoto Y, Uenishi Y, Sunagawa M, Uchiyama T and Yano I: Molecular and supra-molecular structure related differences in toxicity and granulomatogenic activity of mycobacterial cord factor in mice. Microb Pathog 43: 10-21, 2007.
32. Ryll R, Watanabe K, Fujiwara N, Takimoto H, Hasunuma R, Kumazawa Y, Okada M and Yano I: Mycobacterial cord factor, but not sulfolipid, causes depletion of NKT cells and upregulation of CD1d1 on murine macrophages. Microbes Infect 3: 611-619, 2001.
33. Hamasaki N, Isowa K, Kamada K, Terano Y, Matsumoto T, Arakawa T, Kobayashi K and Yano I: In vivo administration of mycobacterial cord factor (Trehalose 6,6'-dimycolate) can induce lung and liver granulomas and thymic atrophy in rabbits. Infect Immun 68: 3704-3709, 2000.
34. Saban MR, Hellmich HL, Simpson C, Davis CA, Lang ML, Ihnat MA, O'Donnell MA, Wu XR and Saban R: Repeated BCG treatment of mouse bladder selectively stimulates small GTPases and HLA antigens and inhibits single-spanning uroplakins. BMC Cancer 7: 204, 2007.

35. Miyazaki J, Kawai K, Kojima T, Oikawa T, Joraku A, Shimazui T, Nakaya A, Yano I, Nakamura T, Harashima H, *et al*: The liposome-incorporating cell wall skeleton of *Mycobacterium bovis* bacillus Calmette-Guéin can directly enhance the susceptibility of cancer cells to lymphokine-activated killer cells through up-regulation of natural-killer group 2, member D ligands. BJU Int 108: 1520-1526, 2011.
36. Chen FH, Crist SA, Zhang GJ, Iwamoto Y and See WA: Interleukin-6 production by human bladder tumor cell lines is up-regulated by bacillus Calmette-Guérin through nuclear factor-kappaB and Ap-1 via an immediate early pathway. J Urol 168: 786-797, 2002.
37. Zhang G, Chen F, Cao Y and See WA: Bacillus Calmette-Guérin induces p21 expression in human transitional carcinoma cell lines via an immediate early, p53 independent pathway. Urol Oncol 25: 221-227, 2007.
38. He C, Jiang H, Geng S, Sheng H, Shen X, Zhang X, Zhu S, Chen X, Yang C and Gao H: Expression and prognostic value of c-Myc and Fas (CD95/APO1) in patients with pancreatic cancer. Int J Clin Exp Pathol 7: 742-750, 2014.
39. Belardelli F and Ferrantini M: Cytokines as a link between innate and adaptive antitumor immunity. Trends Immunol 23: 201-208, 2002.
40. Elsäßer J, Janssen MW, Becker F, Suttmann H, Schmitt K, Sester U, Stöckle M and Sester M: Antigen-specific CD4 T cells are induced after intravesical BCG-instillation therapy in patients with bladder cancer and show similar cytokine profiles as in active tuberculosis. PLoS One 8: e69892, 2013.
41. Ingersoll MA and Albert ML: From infection to immunotherapy: Host immune responses to bacteria at the bladder mucosa. Mucosal Immunol 6: 1041-1053, 2013.
42. Monjazeb AM, Hsiao HH, Sckisel GD and Murphy WJ: The role of antigen-specific and non-specific immunotherapy in the treatment of cancer. J Immunotoxicol 9: 248-258, 2012.
43. Shankaran V, Ikeda H, Bruce AT, White JM, Swanson PE, Old LJ and Schreiber RD: IFNgamma and lymphocytes prevent primary tumour development and shape tumour immunogenicity. Nature 410: 1107-1111, 2001.
44. D'Orazio SE, Halme DG, Ploegh HL and Starnbach MN: Class Ia MHC-deficient BALB/c mice generate $CD8^+$ T cell-mediated protective immunity against *Listeria monocytogenes* infection. J Immunol 171: 291-298, 2003.
45. Kamat AM and Lamm DL: Immunotherapy for bladder cancer. Curr Urol Rep 2: 62-69, 2001.
46. Satyam A, Singh P, Badjatia N, Seth A and Sharma A: A disproportion of TH1/TH2 cytokines with predominance of TH2, in urothelial carcinoma of bladder. Urol Oncol 29: 58-65, 2011.
47. Abadie V, Badell E, Douillard P, Ensergueix D, Leenen PJ, Tanguy M, Fiette L, Saeland S, Gicquel B and Winter N: Neutrophils rapidly migrate via lymphatics after *Mycobacterium bovis* BCG intradermal vaccination and shuttle live bacilli to the draining lymph nodes. Blood 106: 1843-1850, 2005.
48. Luo Y, Chen X, Downs TM, DeWolf WC and O'Donnell MA: IFN-alpha 2B enhances Th1 cytokine responses in bladder cancer patients receiving *Mycobacterium bovis* bacillus Calmette-Guérin immunotherapy. J Immunol 162: 2399-2405, 1999.
49. Böhle A and Brandau S: Immune mechanisms in bacillus Calmette-Guerin immunotherapy for superficial bladder cancer. J Urol 170: 964-969, 2003.
50. Luo Y, Chen X and O'Donnell MA: Role of Th1 and Th2 cytokines in BCG-induced IFN-gamma production: Cytokine promotion and simulation of BCG effect. Cytokine 21: 17-26, 2003.
51. Panaretakis T, Pokrovskaja K, Shoshan MC and Grandér D: Interferon-alpha-induced apoptosis in U266 cells is associated with activation of the proapoptotic Bcl-2 family members Bak and Bax. Oncogene 22: 4543-4556, 2003.
52. Manna SK, Mukhopadhyay A and Aggarwal BB: IFN-alpha suppresses activation of nuclear transcription factors NF-kappa B and activator protein 1 and potentiates TNF-induced apoptosis. J Immunol 165: 4927-4934, 2000.